Available online at www.sciencedirect.com
ScienceDirect
Trans. Nonferrous Met. Soc. China 27(2017) 73−81
Transactions of Nonferrous Metals Society of China
www.tnmsc.cn

Effects of extrusion and heat treatments on microstructure and mechanical properties of Mg−8Zn−1Al−0.5Cu−0.5Mn alloy

Shao-zhen ZHU[1,2], Tian-jiao LUO[1], Ting-an ZHANG[3], Yun-teng LIU[4], Yuan-sheng YANG[1]

1. Institute of Metal Research, Chinese Academy of Sciences, Shenyang 110016, China;
2. School of Materials Science and Engineering, Northeastern University, Shenyang 110819, China;
3. Key Laboratory for Ecological Metallurgy of Multi-metallic Mineral, Ministry of Education, Northeastern University, Shenyang 110819, China;
4. Shandong Key Laboratory for High Strength Lightweight Metallic Materials, Jinan 250014, China

Received 12 December 2015; accepted 1 September 2016

Abstract: The effects of extrusion and heat treatments on the microstructure and mechanical properties of Mg−8Zn−1Al−0.5Cu−0.5Mn magnesium alloy were investigated. Bimodal microstructure is formed in this alloy when it is extruded at 230 and 260 °C, and complete DRX occurs at the extruding temperature of 290 °C. The basal texture of as-extruded alloys is reduced gradually with increasing extrusion temperature due to the larger volume fraction of recrystallized structure at higher temperatures. For the alloy extruded at 290 °C, four different heat treatments routes were investigated. After solution + aging treatments, the grains sizes become larger. Finer and far more densely dispersed precipitates are found in the alloy with solution + double-aging treatments compared with alloy with solution + single-aging treatment. Tensile properties are enhanced remarkably by solution + double-aging treatment with the yield strength, tensile strength and elongation being 298 MPa, 348 MPa and 18%, respectively. This is attributed to the combined effects of fine dynamically recrystallized grains and the uniformly distributed finer precipitates.
Key words: magnesium alloy; extrusion microstructure; texture; heat treatment; mechanical properties

1 Introduction

In the past decades, much attention has been paid to magnesium alloys in transportation, aerospace and 3C industries because of their low density, good castability, high specific strength and specific stiffness [1−3]. Particularly, Mg−Zn series alloys are gradually attracting widespread attention due to their better creep resistance, acceptable castability and low cost. In addition, the Mg−Zn series alloys are age-hardenable, so it is possible to improve their tensile strength by heat treatment. Whereas, the Mg−Zn series alloys have coarse grains and are more sensitive to hot tearing which are unfavorable for warm deformation. In order to refine the microstructure and improve the mechanical properties, expensive elements, such as Zr, Ce [4,5], Bi [6], and Sc [8], have been added into the alloys. However, production costs have also risen. Recently, ZHANG et al [8] have developed a new ZM61 wrought alloy with low cost and high strength, but the elongation of the alloy is below 8%, which has made it inadequate for wide application. Thus, it is necessary to develop a new wrought magnesium alloy with better comprehensive mechanical properties on a cost-effective basis.

Recently, a new high-strength Mg−8Zn−1Al−0.5Cu−0.5Mn magnesium alloy has been developed with addition of cost-effective elements [9]. The addition of Al and Cu can not only accelerate the age-hardening process but also improve the castability of Mg−Zn alloys [10,11]. Mn can improve corrosion resistance by the formation of an intermetallic compound with Fe and increase the fatigue life and tensile strength, especially yield strength [12].

In this work, the Mg−8Zn−1Al−0.5Cu−0.5Mn magnesium alloy was subjected to direct hot extrusion, the microstructure and mechanical properties of as-extruded and heat-treated alloys were investigated, and

Foundation item: Project (2013CB632205) supported by the National Basic Research Program of China; Project (51274184) supported by the National Natural Science Foundation of China
Corresponding author: Yuan-sheng YANG; Tel: +86-24-23971728; Fax: +86-24-23844528; E-mail: ysyang@imr.ac.cn
DOI: 10.1016/S1003-6326(17)60008-6

relevant mechanisms were also discussed in the paper.

2 Experimental

Cast billets of Mg−8.0Zn−1Al−0.5Cu−0.5Mn (mass fraction, %) magnesium alloy (named as ZA81M alloy) were prepared by gravity casting. After solution treatment at 365 °C for 60 h, the billets were air-cooled to room temperature, and then machined to bars with a diameter of 100 mm. The bars were pre-heated to extrusion temperatures (230, 260, 290 °C) and soaked for 2 h prior to extrusion, and then extrusion was carried out at an extrusion ratio of 16 and a ram speed of 3 mm/s.

For the Mg−Zn alloy, the GP zones are formed when the alloys are aged at temperatures of 70−110 °C, and the GP zones are excluded when the temperature is above 110 °C, so 90 °C is selected for the first step aging process in the experiment. The detailed heat treatment parameters of the alloy extruded at 290 °C used in this work are shown in Table 1.

Table 1 Heat treatment parameters for alloys after hot extrusion

Heat treatment process	Solution parameter	Aging parameter
Single aging	−	180 °C, 16 h
Double aging	−	(90 °C, 32 h)+ (180 °C, 8 h)
Solution + single aging	365 °C, 1 h	180 °C, 16 h
Solution + double aging	365 °C, 1 h	(90 °C, 32 h)+ (180 °C, 8 h)

The Philips PW170 X-ray diffractometer was used to identify the phases in the alloy. The textures of the as-extruded alloy were obtained by the D8 Discover X-ray diffractometer. Samples for observation were mechanically polished and then etched in a solution of 4.2 g picric acid + 10 mL water + 10 mL acetic acid + 70 mL ethanol. The microstructures were characterized by optical microscope (OM), scanning electron microscope (JSM−6460) and transmission electron microscope (FEI TECNAI G^2 F20). For mechanical characterization, the dog-bone tensile specimens with a diameter of 5 mm and gage length of 25 mm were measured by AG−100kNG at room temperature with an initial strain rate of 3.0×10^{-3} s^{-1}.

3 Results and discussion

3.1 Microstructure of as-cast and extruded ZA81M alloys

The optical micrographs of ZA81M magnesium alloy in different states are shown in Fig. 1. The as-cast microstructure consists of α-Mg dendrite and eutectic phases dispersed mostly along grain boundaries. After the solution treatment, a few undissolved phases still exist. In ZA81M alloy, the high Zn content (above 6%, mass fraction) that exceeds the maximum solid solubility makes it difficult for complete dissolution of the phases [13], which results in the appearance of a small part of the phases after solution treatment.

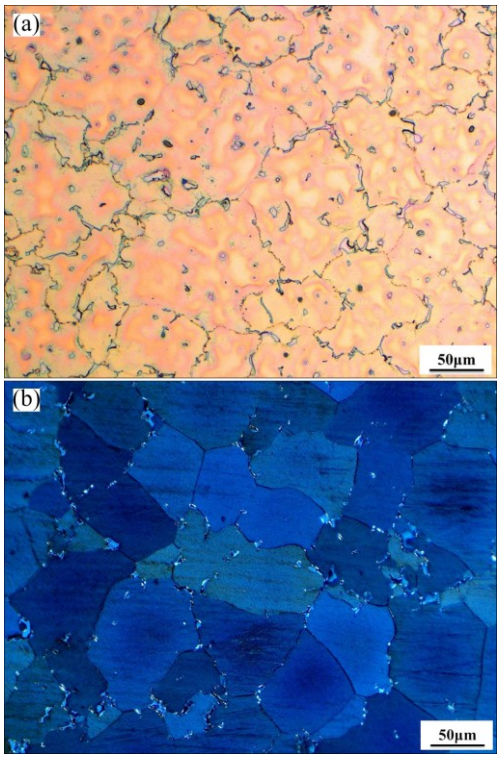

Fig. 1 Optical micrographs of ZA81M magnesium alloy in different states: (a) As-cast; (b) As solution-treated

Figure 2 shows the optical micrographs of the alloys extruded at 230, 260 and 290 °C, respectively. When the alloy is extruded at 230 and 260 °C, it shows the bimodal microstructure, which consists of fine DRX grains (1−3 μm) and some large elongated grains parallel to the extrusion direction. This indicates that dynamic recrystallization has not been completed after hot extrusion. When the alloy was extruded at 290 °C, complete DRX occurs and the alloy has a homogeneous grain structure.

The SEM images of the alloys extruded at different temperatures are shown in Fig. 3. The undissolved phases are broken and routed to the extrusion direction under the compressive stress. Moreover, a large amount of finer precipitates distribute homogeneously in the matrix after extrusion. However, the fine precipitates almost disappear after the solution treatment at 365 °C for 1 h, as shown in Fig. 4.

Figures 5(a)−(c) show the XRD patterns of the as-extruded alloys at different extrusion temperatures. It

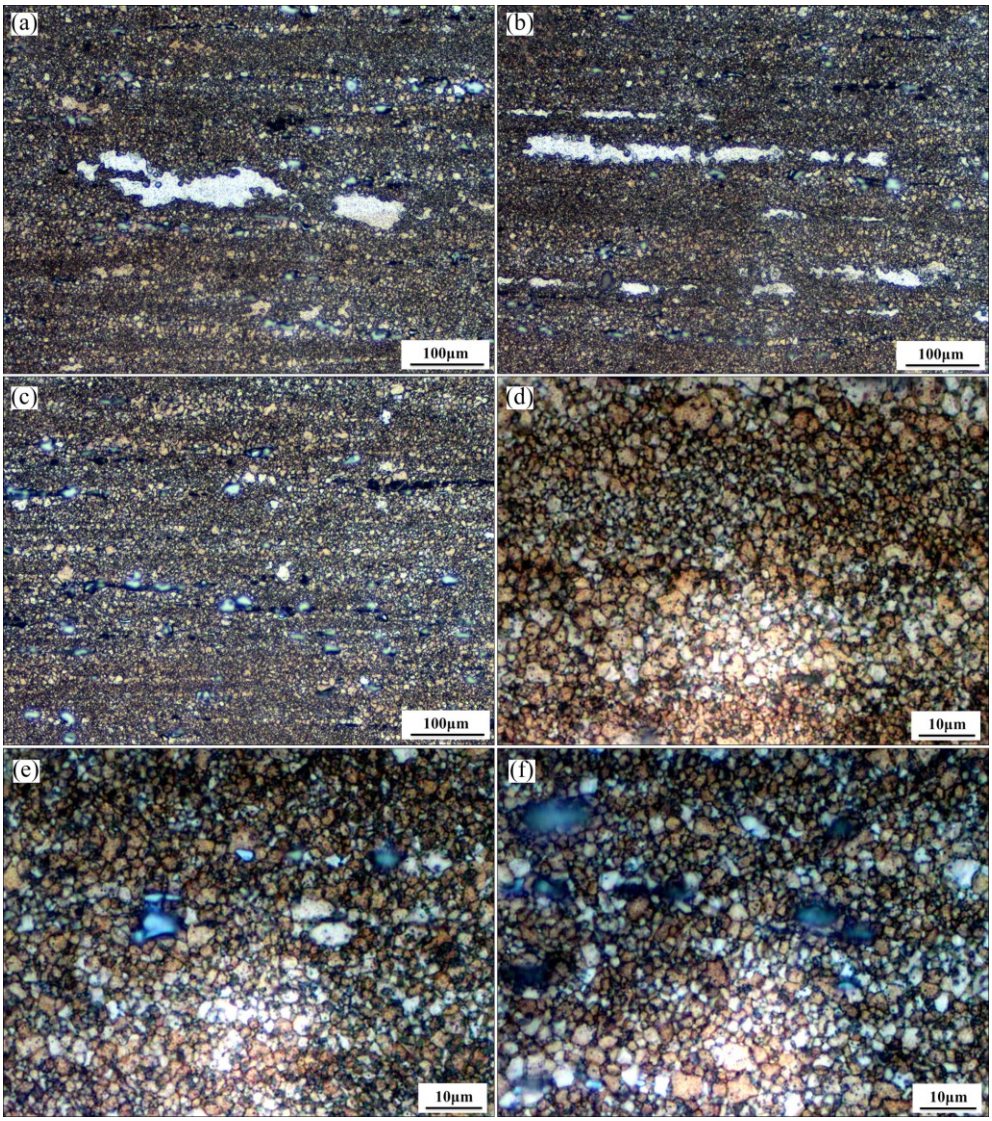

Fig. 2 Optical micrographs of alloys extruded at 230 °C (a, d), 260 °C (b, e) and 290 °C (c, f)

can be seen that the as-extruded alloys are mainly composed of α-Mg, $MgZn_2$ and MgZn phases. Figure 5(d) shows the XRD pattern of the alloy extruded at 260 °C after solution treatment, in addition to α-Mg peak, nearly all other diffraction peaks can be assigned to $MgZn_2$ phase, the diffraction peaks of MgZn phases disappear compared with as-extruded alloys, which agrees well with Fig. 4. According to the above analysis, it can be seen that the coarser precipitate is $MgZn_2$ phase while the finer precipitate is MgZn phase.

Magnesium alloys have poor workability at room temperature due to its hexagonal closed-packed crystal structure with limit number of slip systems. But the workability of magnesium alloys can be increased at elevated temperatures by activating some non-basal slip systems. Generally, the typical extrusion temperature for magnesium alloys is in the range of 300−400 °C [14], whereas the ZA81M magnesium alloy can be smoothly extruded at 230−290 °C and extensive dynamic recrystallization occurs during extrusion process. The enhanced DRX of the ZA81M alloy under low temperature extrusion is largely due to the mechanism of particles stimulated nucleation (PSN) at the widely distributed $MgZn_2$ phases. It has been reported that the coarse particles (d>1 μm) can act as heterogeneous sites for the nucleation of recrystallization by generating local inhomogeneity of the strain energy during the hot extrusion process [15,16]. Meanwhile, many clusters of the large particles are observed in the as-extruded ZA81M alloys, which are known to be more effective than single particles in leading to PSN because of the larger accumulated misorientation. Thus, the widely distributed $MgZn_2$ phases (d>1 μm) may accelerate DRX during hot extrusion process. Also, as shown in Fig. 4(a), fine MgZn phases (300−500 nm) are mostly distributed along DRX grain boundaries. It is well known that fine particles can refine the microstructure by retarding the growth of DRX grains [17], and thereby

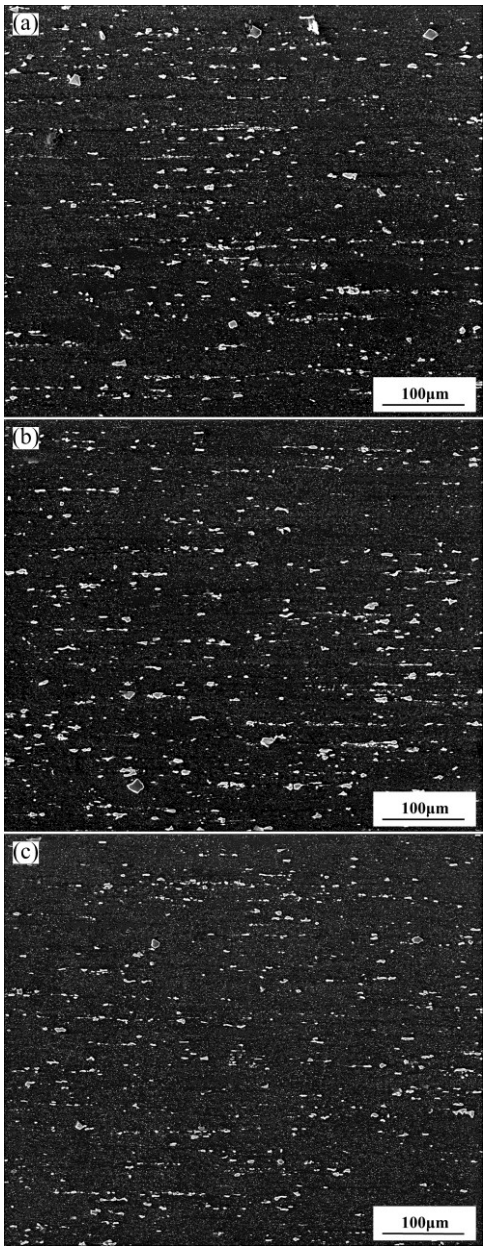

Fig. 3 SEM images of alloys extruded at 230 °C (a), 260 °C (b) and 290 °C (c)

suppressing the grain growth during the dynamic recrystallization.

3.2 Textures of as-extruded ZA81M alloy

Figure 6 shows the pole figures for the as-extruded ZA81M alloy. The {0002} basal texture is formed after hot extrusion process, i.e., the {0002} basal planes and $\langle 10\bar{1}0\rangle$ directions in most grains are distributed parallel to the extrusion direction, which is a typical texture for extruded magnesium alloys.

It can be seen that the intensity of the basal texture of the as-extruded alloy decreases with increasing extrusion temperature, which may result from the relevant DRX process. TONG et al [18] reported that

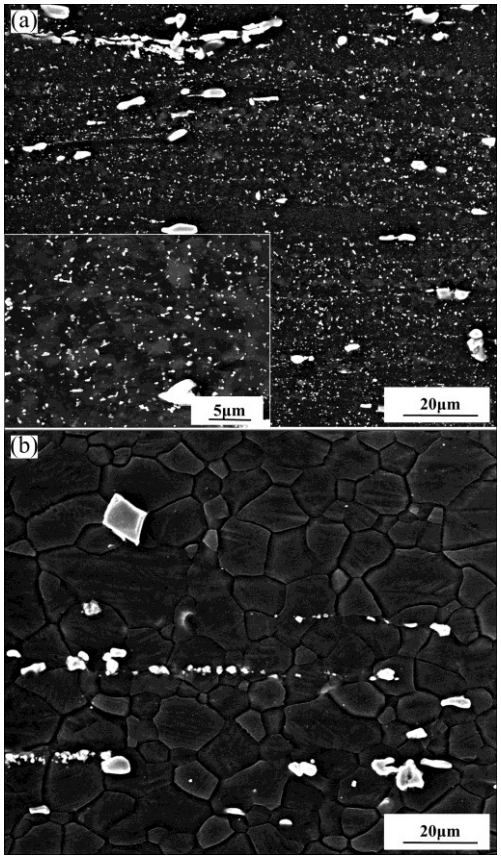

Fig. 4 SEM images of different alloys extruded at 260 °C: (a) As-extruded; (b) As solution-treated at 365 °C for 1 h

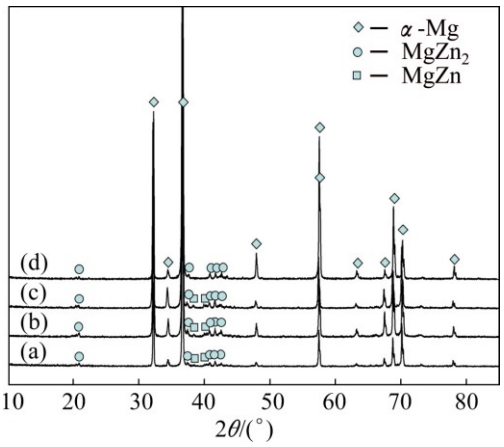

Fig. 5 XRD patterns of alloys extruded under different conditions: (a) Alloy extruded at 230 °C; (b) Alloy extruded at 260 °C; (c) Alloy extruded at 290 °C; (d) Alloy extruded at 260 °C with solution treatment at 365 °C for 1 h

an intensive basal texture was observed in the no-DRX area, whereas the DRX regions represented a dispersive basal texture with the {0002} planes inclining to ED from 0° to 35°. As a consequence, the texture weakening phenomenon is more apparent after extrusion at higher extrusion temperature resulting from the higher volume fraction of the DRX grains.

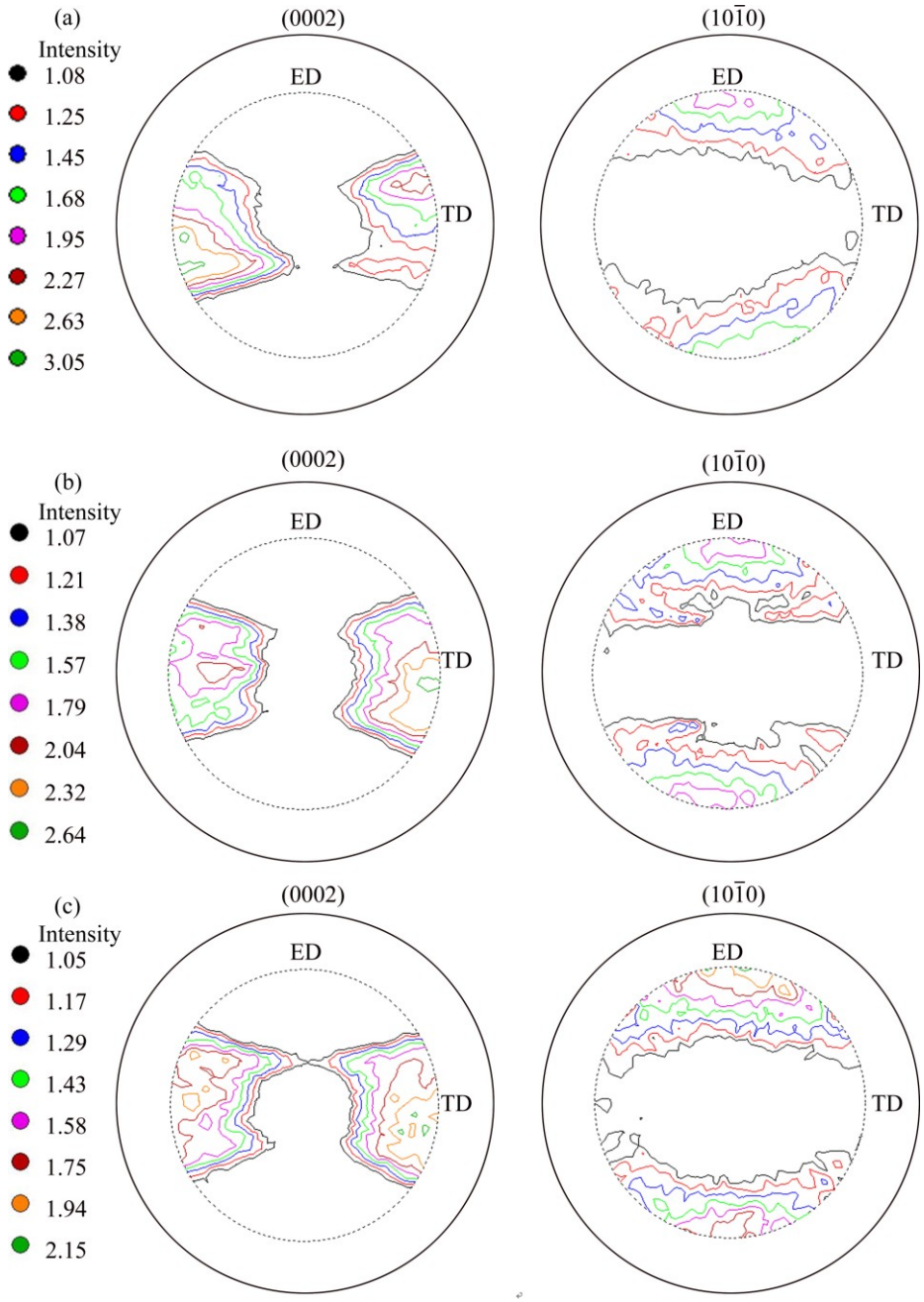

Fig. 6 Pole figures of alloys extruded at 230 °C (a), 260 °C (b) and 290 °C (c)

3.3 Mechanical properties of as-extruded ZA81M alloy

The tensile properties of the as-extruded alloys at different extrusion temperatures are listed in Table 2. In the experiments, extrusion temperatures do not have significant effects on the tensile properties of the as-extruded alloys. The alloy extruded at 290 °C exhibits the relatively optimal comprehensive mechanical properties, the yield strength, ultimate tensile strength and elongation reach 227 MPa, 322 MPa and 23%, respectively.

The microstructure characterization of the as-extruded alloy implies that the main factors for its high tensile strength are the grain refinement and uniformly dispersed secondary phases. The maximum intensity of extrusion texture is only 3.05, suggesting that the effect of this texture on the mechanical properties of

Table 2 Tensile properties of as-extruded alloys at different extrusion temperatures

Extrusion temperature/°C	Yield strength/MPa	Ultimate tensile strength/MPa	Elongation/ %
230	218	317	24
260	218	316	24
290	227	322	23

as-extruded alloy is small. Besides, it is worth noting that the as-extruded alloys have a high elongation to failure. The refinement of the microstructure can be considered as the dominant reason why the alloy shows the excellent ductility at ambient temperature. In addition, the enhanced ductility of the as-extruded alloys can be partly attributed to the low intensity of the extrusion texture.

3.4 Microstructure and mechanical properties of as-aged ZA81M alloy

Figure 7 shows the microstructures of the alloy extruded at 290 °C with different heat treatments. As shown in Fig. 7, by optical microscope, the microstructures of the alloys with direct aging treatments have no obvious change compared with the as-extruded

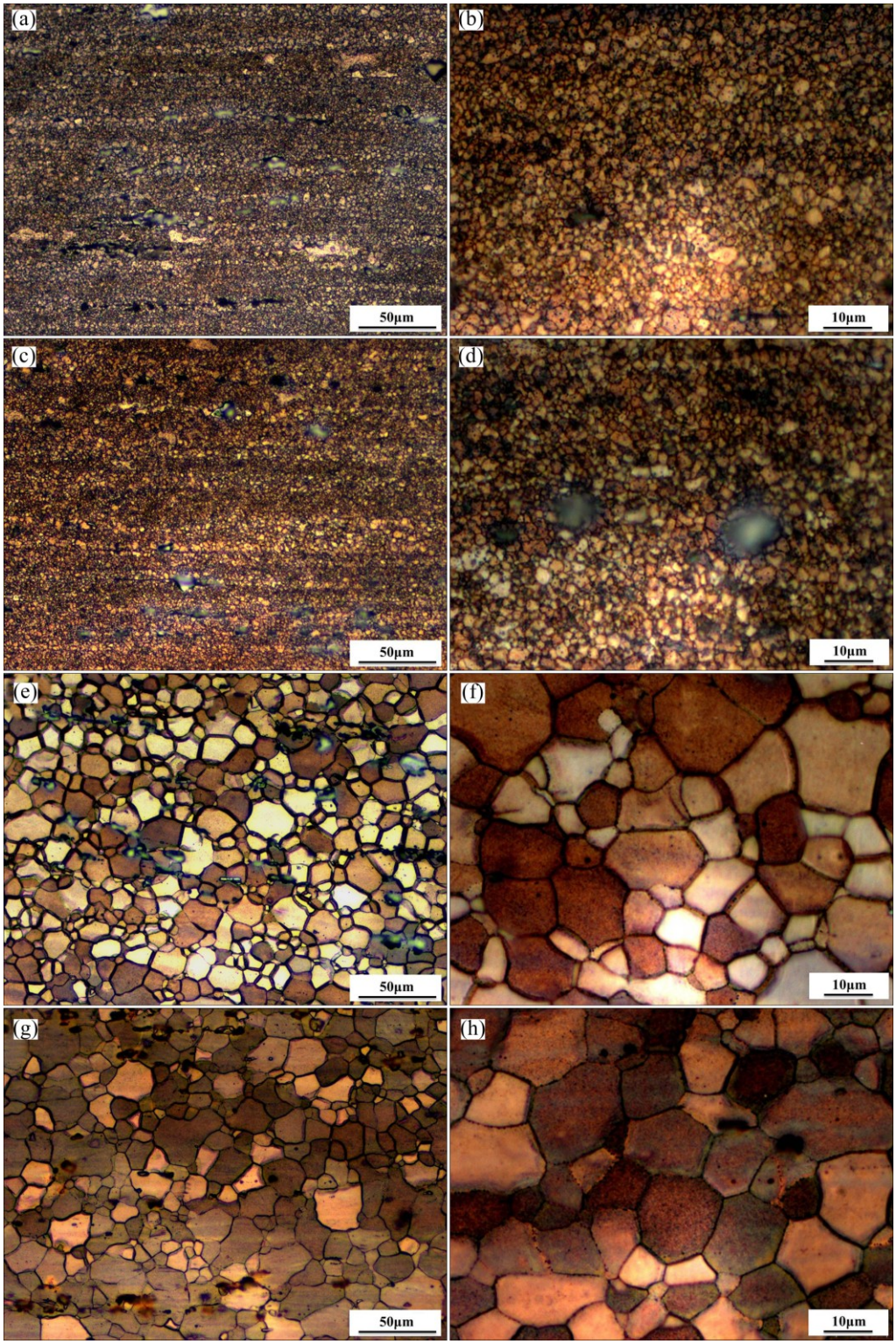

Fig. 7 Optical micrographs of alloys extruded at 290 °C with different heat treatments: (a, b) Direct single-aging; (c, d) Direct double-aging; (e, f) Solution + single-aging; (g, h) Solution + double-aging

microstructures. However, after the solution + aging treatment, the grain size becomes larger obviously.

Representative tensile stress−strain curves of the alloys at room temperature with different heat treatments are shown in Fig. 8 and the mechanical properties of the alloy are summarized in Table 3. It can be seen that, compared with as-extruded alloys, the yield strength of as-aged alloys with direct aging treatment has increased by about 20 MPa, but there is no remarkable change for the ultimate tensile and elongation. However, after solution + aging treatment, the strength of the alloys can be significantly improved, while the elongation decreases obviously. The enhancement of age-hardening response can mainly be attributed to the solution treatment. After the solution heat treatment, all the MgZn phases are dissolved into the matrix, which increases the solid content of Zn in α-Mg matrix, thus improving the age-hardening response during the following aging [19].

Furthermore, the solution + double-aged alloy shows the largest strengthening effect, the ultimate tensile strength, yield strength and elongation reach 348 MPa, 298 MPa and 18%, respectively. The Mg−Zn alloys are well known for their excellent age-hardening response compared with other magnesium alloys. It is generally accepted that the strengthening precipitates in Mg−Zn alloys are β_1' and β_2'. The metastable phase β_1' forms as rods with its long axis parallel to the $[0001]_\alpha$ direction of the α-Mg matrix, while β_2' forms as plates on $(0001)_\alpha$ [18]. According to our previous work, the rod-like precipitate shown in Fig. 9 is β_1' phase [9], which exhibits semi-coherent structure with α-Mg matrix, it could effectively block the basal dislocation slip [19]. It can be seen from Fig. 9 that the precipitates are finer and far more densely dispersed in the alloy with solution + double-aging treatment. This is because in the double-aging treatment, the G. P. zones

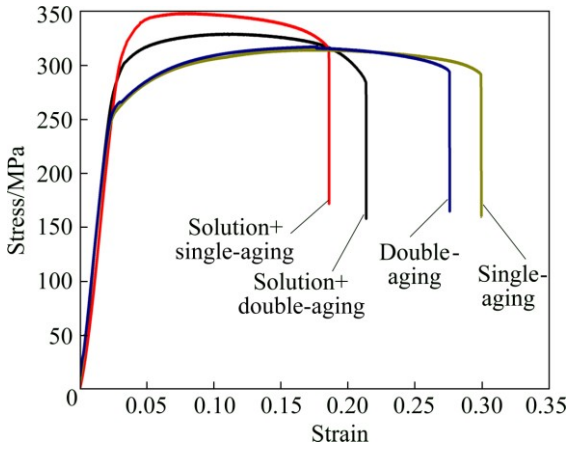

Fig. 8 Representative tensile stress−strain curves at room temperature with different heat treatments

Table 3 Mechanical properties of alloys with various heat treatments

Heat treatment process	Yield strength/MPa	Ultimate tensile strength/MPa	Elongation/%
Single-aging	245	313	25.5
Double-aging	242	312	27.0
Solution + single-aging	263	329	20.0
Solution + double-aging	298	348	18.0

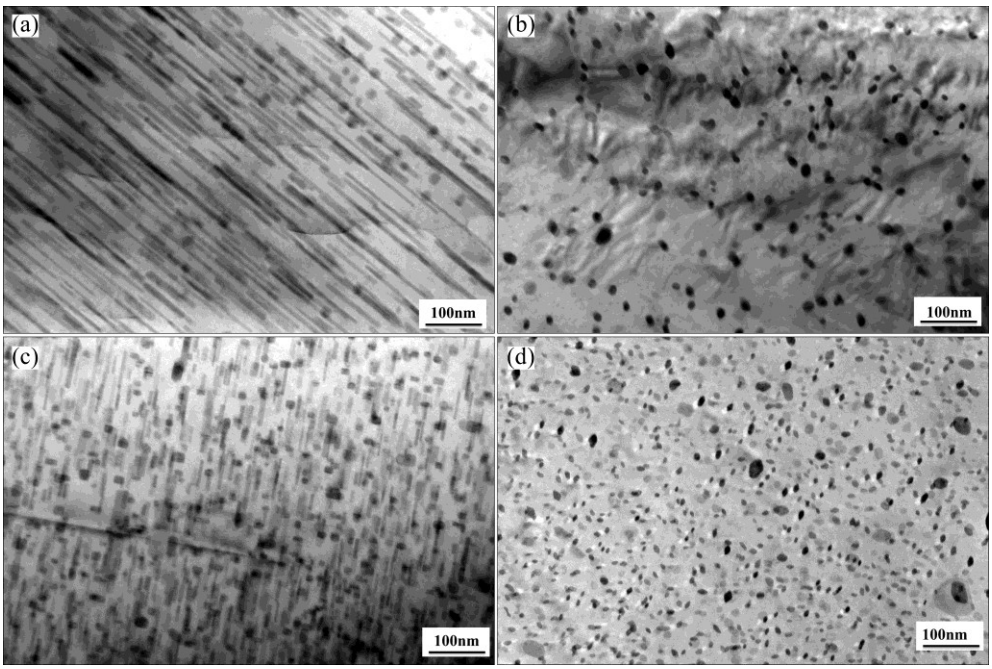

Fig. 9 TEM images of alloys along $[11\bar{2}0]_{Mg}$ (a, c) and $[0001]_{Mg}$ (b, d) under various heat treatments: (a, b) Solution + single-aging; (c, d) Solution + double-aging

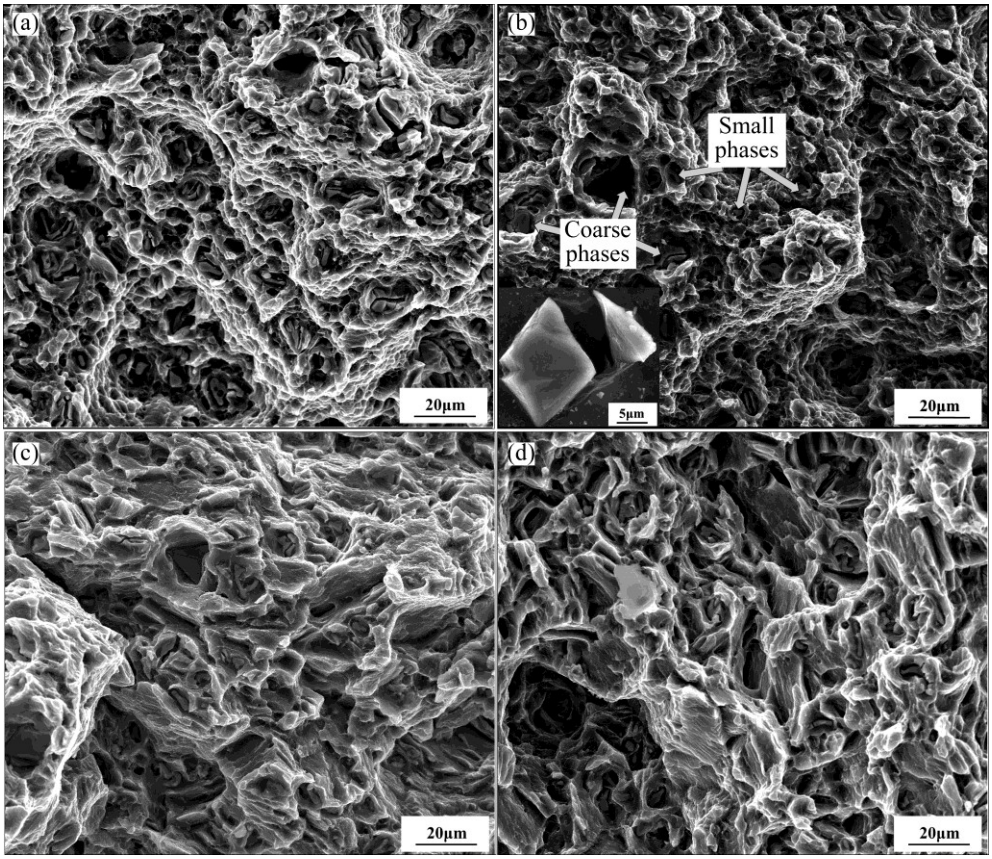

Fig. 10 Tensile fracture surfaces of as-extruded alloys with various heat treatments at room temperature: (a) Single-aging; (b) Double-aging; (c) Solution + single-aging; (d) Solution + double-aging

are formed during the first step aging at the temperature of 90 °C. It is reported that G. P. zones are believed to act as heterogeneous nucleation sites for the transition phase to form, and subsequent aging treatment process, transitional phases precipitate in the zones, which leads to uniform distribution of finer precipitates [10].

Figure 10 shows the SEM images of the tensile fracture surfaces tested at room temperature for the as-aged alloy. It is found that the as-aged alloys with direct aging treatment exhibit predominant dimples which are the feature of ductile fracture. Meanwhile, numerous small phases are located at the bottom of these dimples. It is assumed that coarser phases can act as sites for stress concentration and cavity nucleation due to the pile-up of mobile dislocations during the tensile testing, which tend to generate crack origins [20]. As we can see in Figs. 10(c) and (d), the fracture surface mainly consists of some dimples and tearing ridges. Meanwhile, compared with the as-aged alloys with direct aging treatment, the rapture dimples become shallower and their number becomes smaller, which is in accordance with the poor ductility. This is partly because the nano-sized dispersed precipitates can more effectively hinder the motion of dislocations during deformation. In the meantime, the coarse grains caused by solution treatment also play an important role in reducing ductility of the alloy.

4 Conclusions

1) Bimodal microstructure is observed in the alloys extruded at 230 and 260 °C, and the complete DRX occurs when the alloy is extruded at 290 °C. The average size of the DRX grains is 1−3 μm. The basal texture of the as-extruded ZA81M alloy is reduced gradually with increasing extrusion temperature due to fully dynamic recrystallization at higher temperatures.

2) Extrusion temperature does not have significant effect on the tensile properties of the as-extruded alloy, and the alloy extruded at 290 °C exhibits the relatively optimal comprehensive mechanical properties, the yield strength, ultimate tensile strength and elongation reach 227 MPa, 322 MPa and 23%, respectively.

3) Finer and far more densely dispersed precipitates were found in the alloy with solution + double-aging treatment when compared with alloy with solution + single-aging treatment. The tensile strength is enhanced remarkably by solution + double-aging heat treatment, the yield strength, tensile strength and elongation are 298 MPa, 348 MPa and 18%, respectively, which is

attributed to the combined effects of fine dynamically recrystallized grains and the uniformly distributed finer precipitates.

References

[1] KULEKCI M K. Magnesium and its alloys applications in automotive industry [J]. The International Journal of Advanced Manufacturing Technology, 2008, 39: 851−865.

[2] LUO A A. Magnesium casting technology for structural applications [J]. Journal of Magnesium and Alloys, 2013, 1: 12−22.

[3] PAN Hu-cheng, REN Yu-ping, FU He, ZHAO Hong, WANG Li-qing, MENG Xiang-ying, QIN Gao-wu. Recent developments in rare-earth free wrought magnesium alloys having high strength: A review [J]. Journal of Alloys and Compounds, 2016, 663: 321−331.

[4] PARK S H, YU H, BAE J H, YIM C D, YOU B S. Microstructural evolution of indirect-extruded ZK60 alloy by adding Ce [J]. Journal of Alloys and Compounds, 2012, 545: 139−143.

[5] SELVAN S, RAMANATHAN S. Hot workability of as-cast and extruded ZE41A magnesium alloy using processing maps [J]. Transactions of Nonferrous Metals Society of China, 2011, 21: 257−264.

[6] HUANG Zheng-hua, LIUWANG Han-bo, QI Wen-jun, XU Jing, ZHOU Nan. Effects of Bi on the microstructure and mechanical property of ZK60 alloy [J]. Journal of Magnesium and Alloys, 2015, 3: 29−35.

[7] LIU Ting-ting, PAN Fu-sheng, ZHANG Xi-yan. Effect of Sc addition on the work-hardening behavior of ZK60 magnesium alloy [J]. Materials & Design, 2013, 43: 572−577.

[8] ZHANG Ding-fei, SHI Guo-liang, ZHAO Xia-bing, QI Fu-gang. Microstructure evolution and mechanical properties of Mg−*x*%Zn−1%Mn (*x*=4, 5, 6, 7, 8, 9) wrought magnesium alloys [J]. Transactions of Nonferrous Metals Society of China, 2011, 21: 15−25.

[9] WANG Jing, LIU Rui-dong, LUO Tian-jiao, YANG Yuan-sheng. A high strength and ductility Mg−Zn−Al−Cu−Mn magnesium alloy [J]. Materials & Design, 2013, 47: 746−749.

[10] OH-ISHI K, HONO K, SHIN K S. Effect of pre-aging and Al addition on age-hardening and microstructure in Mg−6wt% Zn alloys [J]. Materials Science and Engineering A, 2008, 496: 425−433.

[11] ZHU H M, SHA G, LIU J W, WU C L, LUO C P, LIU Z W, ZHENG R K, RINGER S P. Microstructure and mechanical properties of Mg−6Zn−*x*Cu−0.6Zr (wt.%) alloys [J]. Journal of Alloys and Compounds, 2011, 509: 3526−3531.

[12] ZHU S M, ABBOTT T B, GIBSON M A, NIE J F, EASTON M A. Age hardening in die-cast Mg−Al−RE alloys due to minor Mn additions [J]. Materials Science and Engineering A, 2016, 656: 34−38.

[13] BALASUBRAMANI N, PILLAI U T S, PAI B C. Optimization of heat treatment parameters in ZA84 magnesium alloy [J]. Journal of Alloys and Compounds, 2008, 457: 118−123.

[14] ZHANG Ding-fei, SHI Guo-liang, DAI Qing-wei, YUAN Wei, DUAN Hong-ling. Microstructures and mechanical properties of high strength Mg−Zn−Mn alloy [J]. Transactions of Nonferrous Metals Society of China, 2008, 18: 59−63.

[15] YU H, KIM Y M, YOU B S, YU H S, PARK S H. Effects of cerium addition on the microstructure, mechanical properties and hot workability of ZK60 alloy [J]. Materials Science and Engineering A, 2013, 559: 798−807.

[16] ROBSON J D, HENRY D T, DAVIS B. Particle effects on recrystallization in magnesium−manganese alloys: Particles-stimulated nucleation [J]. Acta Materialia, 2009, 57: 2739−2747.

[17] JUNG J G, PARK S H, YOU B S. Effect of aging prior to extrusion on the microstructure and mechanical properties of Mg−7Sn−1Al−1Zn alloy [J]. Journal of Alloys and Compounds, 2015, 627: 324−332.

[18] TONG L B, ZHENG M Y, CHENG L R, KAMADO S, ZHANG H J. Effect of extrusion ratio on microstructure, texture and mechanical properties of indirectly extruded Mg−Zn−Ca alloy [J]. Materials Science and Engineering A, 2013, 569: 48−53.

[19] NIE J F. Effects of precipitate shape and orientation on dispersion strengthening in magnesium alloys [J]. Scripta Materialia, 2003, 48: 1009−1015.

[20] HOU Xiu-li, CAO Zhan-yi, ZHAO Lei, WANG Li-dong, WU Yao-ming, WANG Li-ming. Microstructure, texture and mechanical properties of a hot rolled Mg−6.5Gd−1.3Nd−0.7Y−0.3Zn alloy [J]. Materials & Design, 2012, 34: 776−781.

挤压和热处理对 Mg−8Zn−1Al−0.5Cu−0.5Mn 镁合金显微组织和力学性能的影响

朱绍珍[1,2]，罗天骄[1]，张廷安[3]，刘运腾[4]，杨院生[1]

1. 中国科学院 金属研究所，沈阳 110016；2. 东北大学 材料科学与工程学院，沈阳 110819；
3. 东北大学 多金属共生矿生态化冶金教育部重点实验室，沈阳 110819；
4. 山东省轻质高强金属材料省级重点实验室，济南 250014

摘　要：研究挤压和热处理对 Mg−8Zn−1Al−0.5Cu−0.5Mn 镁合金显微组织和力学性能的影响。结果表明，合金在 230 和 260 °C 挤压时呈现双峰组织，而在 290 °C 挤压时合金发生了完全的动态再结晶。随着挤压温度的升高，合金动态再结晶越充分，从而使其基面织构降低。通过研究 4 种不同的热处理制度对 290 °C 下挤压成型合金的影响发现，经过固溶+时效处理后，合金的晶粒发生明显长大。与固溶+单级时效的合金相比，固溶+双级的工艺能显著细化析出相，提高析出相的密度。同时，经固溶+双级时效处理后合金的力学性显著提高，其屈服强度、抗拉强度和伸长率分别为 298 MPa、348 MPa 和 18%，这主要是由细小的再结晶晶粒与均匀弥散分布的第二相共同作用的结果。

关键词：镁合金；挤压组织；织构；热处理；力学性能

(Edited by Wei-ping CHEN)